Transverse stability of solitons and moving domain walls

2000 J. Phys. A: Math. Gen. 33 8105

(http://iopscience.iop.org/0305-4470/33/45/308)

J. Phys. A: Math. Gen. **33** (2000) 8105–8126. Printed in the UK PII: S0305-4470(00)11697-X

Transverse stability of solitons and moving domain walls

H Leblond

Laboratoire POMA, UMR-CNRS 6136, Université d'Angers, 2 B^{d} Lavoisier 49045 Angers Cedex 01, France

Received 4 February 2000, in final form 13 July 2000

Abstract. The effect of transverse perturbations on the domain walls and Nakata's solitons is studied. The integro-differential equation giving an account of this problem is derived using a multiscale expansion. The line-soliton solutions are shown analytically to be unstable with regard to transverse perturbations. Oblique line-soliton interactions, and eventual localized solutions are studied numerically: wave breaking always occurs. This instability gives rise to the emission of a new type of solitary wave.

1. Introduction

The long-wave approximation of electromagnetic waves in ferromagnetic media has been studied by several authors. Two wave types have been identified [1]. They differ by their velocities: one of them, for velocities below some threshold, is yielded by a rotation of the magnetization vector around the propagation axis. In the other type, the magnetization vector oscillates without topological modification of the magnetization field with regard to a uniform steady state. The former wave type is closely related to the relativistic domain walls [2]. In fact, the corresponding soliton is yielded by two parallel moving walls put together.

Each of these wave types can support solitons. Strictly speaking, soliton propagation is a matter of long-distance wave propagation, in which both damping and transverse modulation can be neglected, or at least treated as small perturbations. Two propagation modes giving rise to solitons have been described. They correspond respectively to the two wave types mentioned above, and to the two wave polarizations allowed for oscillatory waves. One of these modes, which had been found by Nakata, is described by the modified Korteweg–de Vries (mKdV) equation [3, 4]. The soliton corresponding to this mode has the above-mentioned structure of two domain walls put together and propagating in a direction perpendicular to their plane. The other mode is more standard: it is given by the propagation of some field perturbation, on the constant background of a saturated magnetization. It obeys the KdV equation and was first derived in [5].

The theory of the propagation of these waves has been developed considering only one space dimension. Their transverse stability has to be studied, together with their oblique interaction and the question of whether localized two- or three-dimensional pulses exist. We study these problems for Nakata's mode, taking into account the inhomogeneous exchange interaction and damping. The model describing the evolution of the wavepacket, taking into account the transverse variations is derived in section 2. It contains a complicated integro-differential term, which implies many difficulties in the treatment of the system. The line solitons are studied in section 3 and are shown to be unstable with regard to transverse

0305-4470/00/458105+22$30.00

perturbations. Other solutions are considered in section 4, still using numerical methods. It is found that the oblique interaction of line-solitons leads to wave breaking, and that it is likely no localized solution exists. The instability can lead to the emission of another solitary wave, as described in section 5.

2. Derivation of a three-dimensional generalization of the mKdV equation

2.1. The model

Wave propagation in ferromagnetic media is described by the so-called Maxwell–Landau model, as follows. The Maxwell equations, assuming a scalar linear relation between the polarization and the electric field, are

$$-\vec{\nabla}(\vec{\nabla}\cdot\vec{H})+\Delta\vec{H}=\frac{1}{c^2}\partial_t^2(\vec{H}+\vec{M}) \tag{1}$$

where $c=\sqrt{\hat{\varepsilon}\mu_0}$ is the speed of light based on the dielectric constant $\hat{\varepsilon}$ of the medium. $\vec{\nabla}=(\partial_x,\partial_y,\partial_z)$ is the spatial gradient operator, $\Delta=(\vec{\nabla})^2$. In this paper, we use either the notation $\partial_t f$ or f_t for the derivative $\frac{\partial f}{\partial t}$ of the function f with regard to the variable t, and so on. As usual, $\vec{H}$ and $\vec{M}$ are the magnetic field and the magnetization density, respectively.

The second equation of the model is the so-called Landau–Lifschitz equation, which, in its most general form, is

$$\partial_t\vec{M}=-\mu_0\delta\vec{M}\wedge\vec{H}_{\text{eff}}+\frac{\sigma}{M}[\vec{M}\wedge(\vec{M}\wedge\vec{H})]. \tag{2}$$

It describes the evolution of the magnetic momentum $\vec{M}$ in the effective magnetic field $\vec{H}_{\text{eff}}$. The second term gives an account of damping, where σ is some negative phenomenological damping constant. The main part of the effective field $\vec{H}_{\text{eff}}$ is the actual field in the medium $\vec{H}$. Several corrective terms can be introduced in $\vec{H}_{\text{eff}}$, in order to give an account of the finite size of the medium (demagnetizing field), anisotropy, and inhomogeneous exchange. We restrict our attention here to isotropic media, for the sake of simplicity. Keeping in mind that the considered field and magnetization are the quantities that exist inside the medium, and considering a sample immersed in some external field strong enough to yield the saturation of the magnetization (even if the saturation is not effectively realized, as it occurs when moving domain walls exist), the demagnetizing field can also be neglected. When considering large wavelengths, the inhomogeneous exchange is also expected to be negligible. But we will see that wave breaking can occur when solving the asymptotic model. It can be thought that this breaking would be prevented by the inhomogeneous exchange, which yields a lower bound for the domain wall size. Therefore the corresponding corrective term has been taken into account. It will be seen that it cannot prevent breaking despite the fact that, from the mathematical point of view, it could stabilize the line-solitons. But the order of magnitude of the inhomogeneous exchange constant β required for this latter effect is unphysical. The effective field is thus

$$\vec{H}_{\text{eff}}=\vec{H}+\beta\Delta\vec{M} \tag{3}$$

where Δ is, as above, the three-dimensional Laplacian operator.

2.2. The scaling

The long-wave and small-amplitude approximation is described through a multiscale formalism. A small parameter ε is introduced, measuring the smallness of the wave amplitude

as well as the largeness of the wave. The magnetization and magnetic fields are expanded in a power series of ε as

$$\vec{M} = \sum_{n \geqslant 0} \varepsilon^n \vec{M}_n \tag{4}$$

$$\vec{H} = \sum_{n \geqslant 0} \varepsilon^n \vec{H}_n. \tag{5}$$

The $\vec{H}_n$ and $\vec{M}_n$ are functions of slow variables ξ, η, ζ, τ defined by

$$\xi = \varepsilon(x - Vt) \qquad \eta = \varepsilon^2 y \qquad \zeta = \varepsilon^2 z \qquad \tau = \varepsilon^3 t. \tag{6}$$

The variable ξ is the longitudinal space variable in a frame moving with the wave. Its scale factor ε gives an account of a long-wave limit, the corresponding wavelength being proportional to $1/\varepsilon$. The wave is slowly modulated in time, depending on the time variable $\tau = \varepsilon^3 t$. Transverse variations must be slow with regard to the ξ variable, so that the propagation direction is still the x-axis, but faster than the τ variable, so that τ can give an account of the evolution of some well-defined three-dimensional wavepacket. Therefore the transverse variables η and ζ are of the order of ε^2.

The external magnetic field creates in the medium some steady state $\vec{M} = \vec{m}$, $\vec{H} = \alpha\vec{m}$, where $\vec{m}$ is some constant vector and α some positive real constant. A remarkable property of Nakata's propagation mode is that it affects the zero order of the expansion, so that $\vec{H}_0$ and $\vec{M}_0$ are not uniformly equal to the steady state $\alpha\vec{m}, \vec{m}$. We assume only that

$$\lim_{\xi \longrightarrow -\infty} \vec{H}_0 = \alpha\vec{m} \qquad \text{and} \qquad \lim_{\xi \longrightarrow -\infty} \vec{M}_0 = \vec{m}. \tag{7}$$

The y-axis is chosen so that the components of $\vec{m}$ are

$$\vec{m} = \begin{pmatrix} m_x \\ m_t \\ 0 \end{pmatrix}. \tag{8}$$

We call φ the angle between this steady-state field and the propagation direction, so that $m_x = m\cos\varphi$ and $m_t = m\sin\varphi$. The terms of higher order are assumed to vanish at infinity.

The effect of damping on the wave under consideration has been studied by Nakata [4] in the $(1 + 1)$-dimensional case. It was treated as a perturbation (σ small). This assumption, which is necessary when studying soliton propagation, is satisfied in real materials. It has been discussed in detail in [6]. As in [4], we set

$$\sigma = \varepsilon\tilde{\sigma} \tag{9}$$

where $\tilde{\sigma}$ is a negative quantity of the order of magnitude of the unity.

Then the expansion is inserted into the Maxwell–Landau equations (1), (2) after rescaling the fields so that the constants c and $\mu_0\delta$ are set equal to one. The coefficients of each power of ε are collected in both members of each equation and equated, and the obtained equations are solved order by order.

2.3. A word about the experimental relevance of this theory

A drawback of this theory is that it concerns long-distance propagation of long waves, while the samples of ferrites used in the experiments are rather small, and many applications require even smaller sizes. A basic question is, to what are the lengths compared, when it is said that they are large. Because the quantity called m in this paper, that is the reduced value of the

saturation magnetization, is of the order of ε^0, it is clear that the length scale associated with this order in the present theory is that of the wavelength corresponding to m:

$$\lambda_0 = \frac{2\pi c}{\delta \mu_0 M_s}. \tag{10}$$

Recall that $c = c_\mathrm{v}/\sqrt{\hat{\varepsilon}_r}$ (c_v is the speed of light in vacuum, $\hat{\varepsilon}_r$ is the relative dielectric constant of the medium) is the speed of light in the medium, and that the magnetization saturation M_s must be replaced by $4\pi M_s$ in CGS units. λ_0 is the wavelength associated with the Larmor frequency. Using the numerical values of [7] for yttrium iron garnet (YIG): $4\pi M_s = 1740$ G and $\hat{\varepsilon}_r = 12$, we obtain $\lambda_0 \simeq 18$ mm. The scale of the pulse length corresponds to the slow variable ξ. It is thus λ_0/ε, and the propagation distance being described by the variable τ, its order of magnitude is that of λ_0/ε^3. Even taking a relatively large value of ε, say $\varepsilon = 1/10$, the pulse length would be measured in units of $\lambda_0/\varepsilon = 18$ cm, and the propagation distance in units of $\lambda_0/\varepsilon^3 = 18$ m. As a matter of comparison the YIG films used to investigate the magnetostatic (MS) solitons in [8] were 15 mm long. Thus, from the very rigorous mathematical point of view, the present theory does not apply to the experimental situations. But in practice, such a rigour may be unnecessary, and we can give several reasons why the results of this paper can be expected to occur at more reasonable length scales.

First, the quantities λ_0/ε and λ_0/ε^3 must be considered as the units of length for the slow variables ξ and τ, respectively. In the numerical computations presented here, the variation range of ξ rarely exceeds two units. A sample length of $2\lambda_0/\varepsilon$, which yields, with the above value, 36 cm, can thus be enough. We can notice further that the values of the slow time τ, for which breaking has been observed in the simulations, are very small: typically from 5×10^{-4} to 2×10^{-2}, the unit for the corresponding propagation distance being λ_0/ε^3. With the above values of the latter, the propagation distance takes values from 9 mm to 36 cm. This first set of considerations reduces the size of the required sample from several tens of metres to several tens of centimetres, which is more reasonable.

Second, there is another choice for λ_0: the wavelength associated with the ferromagnetic resonance frequency. Indeed, the MS spectrum is ordinary given using two characteristic pulsations: ω_H and ω_M [9]. ω_M corresponds to the above-mentioned Larmor frequency, $\omega_H = H_0/\delta\mu_0$ to the ferromagnetic resonance. Consider $\lambda_0' = \frac{2\pi c}{\delta \mu_0 H_0}$; obviously, $\lambda_0' = \lambda_0'/\alpha$. Thus, using a large value of α decreases λ_0', and consequently the pulse length and propagation length can be reduced. As an example, using $\alpha = 20$, that is an external field of 34 800 Oe, reduces the above value of the required sample length to $2\lambda_0'/\varepsilon = 18$ mm, which is close to the usual experimental values.

We must admit that these considerations are not correct from the purely mathematical point of view, because they use a value of alpha greater than $1/\varepsilon$, and involve values of τ very small with regard to ε and even ε^2. In such a case, the parameter ε can no longer be considered as a perturbative parameter, but only as an order parameter that allows us to formally isolate a given phenomenon. The main difference, apart from the mathematical rigour, is that the phenomenon isolated theoretically in such an artificial way arises experimentally together with the other ones. But, despite this drawback, many theoretical works based on such an approach have already given good results.

Thus this paper, that is fully correct from the mathematical point of view in physical situations that are rather far from the usual experimental situations, can be expected to give a correct account of the latter, despite that mathematical rigour is not completely satisfied in this case.

2.4. Resolution of the perturbative scheme

2.4.1. Order zero. Equation (2) at order ε^0 shows that $\vec{M}_0$ and $\vec{H}_0$ must be collinear. Equation (1) at order ε^2 yields, after integrating twice with regard to ξ: $M_0^x = -H_0^x$, and $M_0^s = -\gamma H_0^s$ for $s = y, z$, with $\gamma = 1 - 1/V^2$ (the integration constants are all zero because all field components vanish at infinity). Then equation (2) at order ε^1 reduces to $M_0^x = 0$, and $(1 + \alpha\gamma)M_0^s = 0$ (for $s = y, z$). Nakata's mode corresponds to the solution of this latter equation where $(1 + \alpha\gamma) = 0$, and M_0^y and M_0^z are free. This allows the determination of the speed V:

$$V = \sqrt{\frac{\alpha}{1+\alpha}}. \tag{11}$$

It is the limit of both the group velocity $\frac{\mathrm{d}\omega}{\mathrm{d}k}$ and the phase velocity $\frac{\omega}{k}$ of the 'acoustic' wave with positive helicity, when the pulsation ω and the wavevector k tend to zero. The long-wave limit of the velocity of the wave with negative helicity is $V' = \sqrt{\frac{\alpha+\sin^2\varphi}{1+\alpha}}$. The evolution of the corresponding long-wave propagation mode is governed by the KdV equation [5]. It follows from equation (2) that $\vec{M}$ has a constant norm, and so does $\vec{M}_0$. It is thus

$$\vec{M}_0 = \begin{pmatrix} m_x \\ m_t \cos\theta \\ m_t \sin\theta \end{pmatrix} \tag{12}$$

$\vec{H}_0 = \alpha M_0$ and $\lim_{\xi \longrightarrow -\infty} \theta = 0$. Nakata showed that, neglecting transverse variations and inhomogeneous exchange interaction, $v = \partial_\xi \theta$ obeys the mKdV equation. The three-dimensional evolution of the function θ is the concern of this paper.

2.4.2. Order one. Equation (1) at order ε^3 yields, after integration, $M_1^s = -\gamma H_1^s$, $(s = y, z)$, and

$$M_1^x = -H_1^x - \frac{\alpha m_t}{V^2} \int_{-\infty}^{\xi} (\partial_\eta \cos\theta + \partial_\zeta \sin\theta)\, \mathrm{d}\xi'. \tag{13}$$

Then equation (2) at order ε^1 yields, besides the compatibility condition that $||\vec{M}_0||$ is a constant, mentioned above, trivial equations for H_1^y and H_1^z and

$$H_1^x = \frac{-V}{1+\alpha}\theta_\xi - \alpha m_t \int_{-\infty}^{\xi} (\partial_\eta \cos\theta + \partial_\zeta \sin\theta)\, \mathrm{d}\xi'. \tag{14}$$

2.4.3. Order two. Equation (1) at order ε^4 yields

$$M_2^y = -\gamma H_2^y + (1+\alpha) m_t \int_{-\infty}^{\xi} \int_{-\infty}^{\xi'} (\partial_\eta^2 + \partial_\zeta^2) \cos\theta \, \mathrm{d}\xi' \, \mathrm{d}\xi'' + \frac{1}{V(1+\alpha)}\theta_\eta + \frac{2(1+\alpha)m_t}{V} \int_{-\infty}^{\xi} \partial_\tau \cos\theta \, \mathrm{d}\xi' \tag{15}$$

$$M_2^z = -\gamma H_2^z + (1+\alpha) m_t \int_{-\infty}^{\xi} \int_{-\infty}^{\xi'} (\partial_\eta^2 + \partial_\zeta^2) \sin\theta \, \mathrm{d}\xi' \, \mathrm{d}\xi'' + \frac{1}{V(1+\alpha)}\theta_\zeta + \frac{2(1+\alpha)m_t}{V} \int_{-\infty}^{\xi} \partial_\tau \sin\theta \, \mathrm{d}\xi'. \tag{16}$$

Equation (2) at order ε^2 is

$$V \partial_\xi \vec{M}_1 = \vec{M}_0 \wedge (\vec{H}_2 - \alpha \vec{M}_2) + \vec{M}_1 \wedge \vec{H}_1 + \beta \vec{M}_0 \wedge \partial_\xi^2 \vec{M}_0 - \frac{\tilde{\sigma}}{m} \vec{M}_0 \wedge (\vec{M}_0 \wedge (\vec{H}_1 - \alpha \vec{M}_1)). \tag{17}$$

The x component of $\vec{M}_1 \wedge \vec{H}_1$ is zero, and that of the inhomogeneous exchange term $\beta \vec{M}_0 \wedge \partial_\xi^2 \vec{M}_0$ is simply $\beta m_t^2 \theta_{\xi\xi}$. The x component of the left-hand side term is given by equation (13), and that of the first term on the right-hand side is computed from equations (15) and (16). Then the x component of equation (17) yields the required evolution equation for θ. This equation is studied in the next section.

2.5. A three-dimensional mKdV equation

2.5.1. The coefficients of the equation. The evolution equation for the angle θ or its derivative v is the x component of equation (17). It is

$$\begin{aligned}\mu \partial_\xi^2 \theta + \gamma \partial_\xi \theta = {} & \sin\theta \int_{-\infty}^{\xi} \partial_\tau \cos\theta \, \mathrm{d}\xi' - \cos\theta \int_{-\infty}^{\xi} \partial_\tau \sin\theta \, \mathrm{d}\xi' \\ & + \rho \Bigg(\sin\theta \int_{-\infty}^{\xi} \int_{-\infty}^{\xi'} (\partial_\eta^2 + \partial_\zeta^2) \cos\theta \, \mathrm{d}\xi' \, \mathrm{d}\xi'' \\ & - \cos\theta \int_{-\infty}^{\xi} \int_{-\infty}^{\xi'} (\partial_\eta^2 + \partial_\zeta^2) \sin\theta \, \mathrm{d}\xi' \, \mathrm{d}\xi'' \Bigg) \end{aligned} \tag{18}$$

with

$$\mu = \frac{\sqrt{\alpha}}{2(1+\alpha)^{7/2} m^2 \sin^2\varphi} - \frac{\beta}{2\sqrt{\alpha}(1+\alpha)^{3/2}} \tag{19}$$

$$\gamma = \frac{\tilde{\sigma}}{2m(1+\alpha)^2} \tag{20}$$

$$\rho = \frac{V}{2} = \frac{1}{2}\sqrt{\frac{\alpha}{1+\alpha}}. \tag{21}$$

The inhomogeneous exchange interaction intervenes only through a modification of the expression of the coefficient μ, with regard to the value obtained by Nakata, that is found again when setting $\beta = 0$. When inhomogeneous exchange is negligible ($\beta = 0$), the coefficient μ is always positive. If β is large enough, μ can be negative. Precisely, μ becomes negative when β is larger than $\beta_0 = \alpha((1+\alpha)m \sin\varphi)^{-2}$, or, for a given value of β, less than $\frac{1}{4}(m \sin\varphi)^{-2}$, μ becomes negative when either $\alpha < \alpha_-$ or $\alpha > \alpha_+$, with $\alpha_\pm = \frac{1}{2\tilde{\beta}}(1 - 2\tilde{\beta} \pm \sqrt{1-4\tilde{\beta}})$, where $\tilde{\beta} = \beta m^2 \sin^2\varphi$. The experimental values are such that this never occurs. Indeed, a typical value of β is, for YIG, $\beta = 3.1 \times 10^{-12}$ cm^2. With the above-mentioned value of the saturation magnetization of YIG (1740 Oe), $m = 353$ m^{-1}, and $\tilde{\beta} \simeq 4 \times 10^{-11}$ even with $\varphi = \pi/2$. Then $\alpha_- \simeq 4 \times 10^{-11}$ and $\alpha_+ \simeq 0.25 \times 10^{11}$ are not accessible values. Thus μ is always positive in practice. At least for the considered material, inhomogeneous exchange is, in fact, completely negligible in the present problem. It is easily seen from expression (21) of ρ that this coefficient is always positive.

2.5.2. Expressions of the transverse dependency term. More complicated is the dependency with regard to the transverse variables η and ζ, involving two integrations with regard to ξ. The transformation found by Nakata, to reduce the one-dimensional equation analogous to equation (18) to an mKdV equation, works only partially in the present case. Let us clarify it: we denote by C and S the following integrals:

$$C = \int_{-\infty}^{\xi} (\partial_\eta^2 + \partial_\zeta^2) \cos\theta \, \mathrm{d}\xi' \tag{22}$$

$$S = \int_{-\infty}^{\xi} (\partial_\eta^2 + \partial_\zeta^2) \sin\theta \, \mathrm{d}\xi'. \tag{23}$$

Taking the derivative of equation (18) with regard to ξ yields

$$\mu\theta_{\xi\xi\xi}+\gamma\theta_{\xi\xi}=\theta_\xi\Bigg[\cos\theta\int_{-\infty}^{\xi}\partial_\tau\cos\theta\,\mathrm{d}\xi'+\sin\theta\int_{-\infty}^{\xi}\partial_\tau\sin\theta\,\mathrm{d}\xi' +\rho\Bigg(\cos\theta\int_{-\infty}^{\xi}C\,\mathrm{d}\xi'+\sin\theta\int_{-\infty}^{\xi}S\,\mathrm{d}\xi'\Bigg)\Bigg]-\theta_\tau+\rho(\sin\theta C-\cos\theta S). \tag{24}$$

The factor of θ_ξ is isolated and its derivative is taken once again:

$$\partial_\xi\left(\frac{\theta_\tau+\mu\theta_{\xi\xi\xi}+\gamma\theta_{\xi\xi}-\rho(\sin\theta C-\cos\theta S)}{\theta_\xi}\right)=\rho(\cos\theta C+\sin\theta S) +\theta_\xi\Bigg[-\sin\theta\int_{-\infty}^{\xi}\partial_\tau\cos\theta\,\mathrm{d}\xi'+\cos\theta\int_{-\infty}^{\xi}\partial_\tau\sin\theta\,\mathrm{d}\xi' +\rho\Bigg(-\sin\theta\int_{-\infty}^{\xi}C\,\mathrm{d}\xi'+\cos\theta\int_{-\infty}^{\xi}S\,\mathrm{d}\xi'\Bigg)\Bigg]. \tag{25}$$

Identifying the factor of θ_ξ on the right-hand side of equation (25) with the right-hand side of equation (18), integrating once, and multiplying by θ_ξ yields

$$\theta_\tau+\mu\theta_{\xi\xi\xi}+\frac{\mu}{2}(\theta_\xi)^3=-\gamma\left(\theta_{\xi\xi}+\theta_\xi\int_{-\infty}^{\xi}\theta_\xi^2\,\mathrm{d}\xi'\right) +\rho\left(\theta_\xi\int_{-\infty}^{\xi}(\cos\theta C+\sin\theta S)\,\mathrm{d}\xi'-(\cos\theta S-\sin\theta C)\right). \tag{26}$$

Equation (26) is thus integro-differential. The term with the coefficient γ proportional to the damping constant σ gives an account of damping, which had already been found in [4]. The transverse dependency is taken into account by the second term on the right-hand side. Indeed, the second transverse derivatives appear in the expressions of C and S. This transverse term is not only integro-differential, but also involves the non-algebraic functions sine and cosine.

Setting $\Psi=\sin\theta S+\cos\theta C$ and $\Phi=\cos\theta S-\sin\theta C$ yields the following three-field system, equivalent to equation (26)

$$\theta_\tau+\mu\theta_{\xi\xi\xi}+\frac{\mu}{2}(\theta_\xi)^3=-\gamma\theta_{\xi\xi}-\rho\Phi+\theta_\xi\int_{-\infty}^{\xi}(\rho\Psi-\gamma\theta_\xi^2)\,\mathrm{d}\xi' \tag{27}$$

$$\Psi_\xi=\Phi\theta_\xi-(\theta_\eta^2+\theta_\zeta^2) \tag{28}$$

$$\Phi_\xi=-\Psi\theta_\xi+\theta_{\eta\eta}+\theta_{\zeta\zeta}. \tag{29}$$

Making use of the unknown function $F=\int_{-\infty}^{\xi}\Psi\,\mathrm{d}\xi'$ instead of Ψ, the transverse dependency in the system (27)–(29) becomes purely differential. Taking the derivative of equation (26) with regard to ξ yields the following evolution equation for the ξ derivative v of θ, ($v=\theta_\xi=\partial_\xi\theta$):

$$v_\tau+\mu v_{\xi\xi\xi}+\tfrac{3}{2}\mu v^2v_\xi-\rho\left(v_\xi\int_{-\infty}^{\xi}\Psi\,\mathrm{d}\xi'+2v\Psi\right)=-\rho\int_{-\infty}^{\xi}(\partial_\eta^2+\partial_\zeta^2)v\,\mathrm{d}\xi' -\gamma\left(v_{\xi\xi}+v_\xi\int_{-\infty}^{\xi}v^2\,\mathrm{d}\xi'+v^3\right). \tag{30}$$

2.5.3. Relations with the Kadomtsev–Petviashvili (KP) equation. Equation (30) is a three-dimensional generalization of the mKdV equation:

$$v_\tau+\mu v_{\xi\xi\xi}+\tfrac{3}{2}\mu v^2v_\xi=0. \tag{31}$$

Leaving aside the damping term, and the terms involving Ψ, equation (30) is also comparable to the KP equation, which is, using the same notation as in the present physical case for the function, variables and coefficients,

$$(v_\tau + \mu v_{\xi\xi\xi} + \tfrac{3}{2}\mu v v_\xi)_\xi = -\rho v_{\eta\eta}. \tag{32}$$

When the product $\mu\rho$ of the coefficients is negative, equation (32) is the KP I equation, that admits lump solutions, algebraically decaying in all directions, but for which the line-solitons are unstable. When $\mu\rho$ is positive, it is the so-called KP II equation, without lump solutions, but for which line-solitons are stable [10]. Here $\mu\rho$ is almost always positive, but it will be seen that the above-mentioned conclusions regarding the KP II equation are also not true for equation (30). The latter differs from the KP equation on three points. First, the nonlinear term is, as is obvious from the one-dimensional case, that of the mKdV equation. Second, the KP equation gives no account of the damping. Third, equation (30) involves not only the simple transverse dependency through $v_{\eta\eta}$, but also an integro-differential term involving the function Ψ.

The simplest three-dimensional generalization of the mKdV equation (31) is obtained by using the same transverse dependency as in the KP equation (32). It is, with the present notations,

$$v_\tau + \mu v_{\xi\xi\xi} + \tfrac{3}{2}\mu v^2 v_\xi = -\rho \int_{-\infty}^{\xi} (v_{\eta\eta} + v_{\zeta\zeta})\, \mathrm{d}\xi'. \tag{33}$$

We can call equation (33) the ((3 + 1)-dimensional) modified Kadomtsev–Petviashvili (mKP) equation. It must be noticed that the mKP equation is not integrable by means of the inverse scattering transform (IST) method. There exists some (2 + 1)-dimensional generalizations of the mKdV equation that are completely integrable, and may also be called mKP [10]. Unfortunately, equation (30) does not coincide with any of these equations.

3. Solitons and moving walls

3.1. Self-similar solutions and damping

The soliton solution of the mKdV equation, obtained by neglecting both damping and transverse modulation in equation (30), is given in [3]. It corresponds to a complete revolution of the magnetization density about the propagation direction (typically, θ increases from 0 to 2π). It propagates without deformation under the above assumption, in particular $\sigma = 0$. When $\sigma \neq 0$, damping obviously modifies the propagation, leading to a narrowing of the pulse, and blowing up of the derivative v of the angle θ. It can seem strange that blow-up follows from absorption, but in fact here it corresponds to a state of lower energy. Indeed, the magnetic energy is contained in the region where the magnetization is antiparallel to the magnetic field. The smaller this region is, the lower the energy is, and the size of this region is that of the pulse. When the derivative v increases, so does the energy due to the inhomogeneous exchange interaction. But the latter is always very small in the frame of the long-wave approximation.

On the other hand, the moving domain wall, which is a solution of the same equation corresponding to a half turn of the magnetization vector (θ increases from 0 to π), is not a self-similar solution of the mKdV equation: wave breaking occurs. But it can be stabilized by the damping, in a way analogous to the regularization of the shock wave by damping described by the Burgers' equation [11]. These steady-state solutions are roughly described by the following analytic expression [2]:

$$v = \frac{\lambda}{\cosh(\lambda\xi - \mu\lambda^3\tau)}. \tag{34}$$

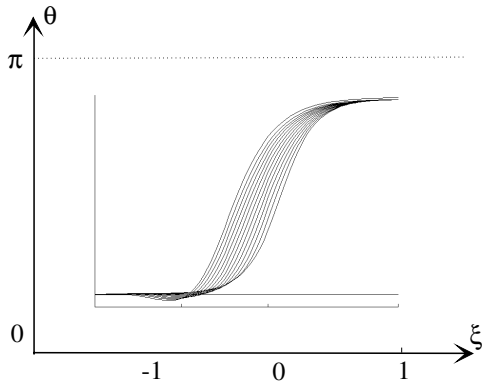

Figure 1. Plot of the precession angle θ against the propagation variable ξ for various values of the time τ, showing the stabilization of the domain wall profile, that moves to the left in the moving frame of the plot. $\mu = 1$, $\rho = 1/4$, $\gamma = -5$. Plotted at times $\tau = 0$, 0.002, 0.004, and so on up to 0.030. Initial data: $v = 4/\cosh(4(\xi - 0.1) + 2\eta)$.

Apart from the propagation term, expression (34) coincides with the classical one for a domain wall given by Landau [12]. Using expression (34) as the initial data in the numerical resolution of equation (30) allows us to check this statement, as shown in figure 1.

3.2. The line-solitons

3.2.1. Analytic expression. We discuss more precisely in the present section the first of the two types of self-similar solutions presented above, called solitons. As mentioned above, they are stable only if damping is negligible, precisely: $\sigma \in \mathrm{O}(\varepsilon^2)$, so that $\tilde{\sigma} = 0$ and γ, given by equation (20), is zero. Therefore we make this assumption in this section. We make use of the traditional term 'line-soliton' corresponding to a two-dimensional situation, although the present one is three dimensional, and the less usual term 'plane soliton' would be more appropriate.

The function Ψ involved in equation (30) is

$$\Psi = \sin\theta \int_{-\infty}^{\xi} (\partial_\eta^2 + \partial_\zeta^2) \sin\theta \, \mathrm{d}\xi' + \cos\theta \int_{-\infty}^{\xi} (\partial_\eta^2 + \partial_\zeta^2) \cos\theta \, \mathrm{d}\xi'. \tag{35}$$

Looking for a quasi-one-dimensional solution $v = v(\xi + b\eta + c\zeta)$ it is easily seen that $\Psi \equiv 0$. Thus, in this special situation, equation (30) coincides exactly with the mKP equation (33). Then the change of variables:

$$\begin{aligned} \tilde{\xi} &= \xi + b\eta + c\zeta - \rho(b^2 + c^2)\tau \\ \tilde{\tau} &= \tau \end{aligned} \tag{36}$$

reduces equation (30) to the mKdV equation:

$$v_{\tilde{\tau}} + \mu v_{\tilde{\xi}\tilde{\xi}\tilde{\xi}} + \tfrac{3}{2}\mu v^2 v_{\tilde{\xi}} = 0. \tag{37}$$

The soliton solution of equation (37) is

$$v = \frac{2\lambda}{\cosh(\lambda\tilde{\xi} - \mu\lambda^3\tilde{\tau})}. \tag{38}$$

With the above definition of the $\tilde{\xi}$ variable, this yields a solitary wave solution of both equations (30) and (33), analogous to the line-soliton of the KP equation. The corresponding angle θ is

$$\theta = \pi + 4 \arctan\tanh\left[\frac{\lambda}{2}(\xi + b\eta + c\zeta - (\rho(b^2 + c^2) + \mu\lambda^2)\tau)\right]. \tag{39}$$

3.2.2. Soliton stability. The stability of the line-soliton can be studied using the approach of [13, p 259 *sq.*]. The soliton is perturbed transversely in the following way. It has the expression

$$v^{(0)} = 2\lambda \operatorname{sech}(\lambda\xi - \mu\lambda^3\tau - \lambda\xi^{(0)}) \tag{40}$$

where $\xi^{(0)}$ can evolve slowly in time and in the transverse direction. Precisely, $\xi^{(0)} = \xi^{(0)}(T, Y)$, with

$$T = \delta\tau \qquad \text{and} \qquad Y = \delta\eta \tag{41}$$

δ being some small parameter. We set

$$X = \xi - \mu\lambda^2\tau - \xi^{(0)} \tag{42}$$

and, according to the principles of the multiscale formalism, expand the solution v of equation (30) into $v = v^{(0)} + \delta v^{(1)} + \delta^2 v^{(2)} + \cdots$, where the functions $v^{(1)}, v^{(2)}, \ldots$ depend on the three variables X, T, Y, defined by (41) and (42), considered as independent variables. The detail of the proof is given in appendix A. At order δ^2 is obtained the evolution equation for $\xi^{(0)}$, which is

$$\xi^{(0)}_{TT} - 4\mu\rho\lambda^2 \frac{J}{J_0} \xi^{(0)}_{YY} = 0 \tag{43}$$

where $J_0 = \int_{-\infty}^{+\infty} {v^{(0)}}^2 \, \mathrm{d}X'$, and J is given by equation (69) in appendix A. Using the explicit expression (38) of $v^{(0)}$, we get $J = -J_0 = -8\lambda$, and equation (43) describes an instability when $\mu\rho$ is positive, while $\xi^{(0)}$ remains bounded when $\mu\rho$ is negative.

The same reasoning, made on the mKP equation (33), leads to the same evolution equation (43), but with J replaced by J_0. The sign in (43) is thus changed, and stability occurs for $\mu\rho > 0$, as for the KP II equation. The conclusions are thus inverted. The physical value of $\mu\rho$ is positive, and thus the line-solitons are not stable. By analogy with the KP I equation, it can be thought that this instability may lead to the formation of localized solutions, comparable to the lump solutions of KP I. We will see below that this is not the case, and that another instability mechanism occurs. It must be noticed that the change in the stability condition for equation (30) is due the Ψ term, involving the functions sine and cosine. This means that the instability is due to the proper structure of the considered type of wave, involving a rotation of the magnetization around the z-axis.

3.2.3. Linear stability. We consider the stability of some line-soliton $v^{(0)}$ through the influence of some small perturbation $v^{(1)}$, rapidly oscillating with regard to η. The equations of the linear stability analysis are easily derived but, due to the integrations with regard to ξ, they cannot be solved explicitly. We thus employ a numerical approach as follows: the considered initial data $v_0 = v_0^{(0)} + v_0^{(1)}$ is

$$v_0 = \frac{2b}{\cosh(b(x - x_0) + cy)} (1 + g\cos(ly)) \tag{44}$$

so that $v_0^{(1)} = v_0^{(0)} g \cos ly$. Numerical resolution of equation (30) shows that the oscillations are amplified when ρ is negative, and damped when ρ is positive. This result does not depend on the sign of the dispersion constant μ. It is shown in figures 2(*b*) and (*c*).

It is worth considering the same stability problem for the mKP equation (33). We seek for a solution $v = v^{(0)} + f(\xi, \tau)\mathrm{e}^{\mathrm{i}k\eta}$ of (33), and see easily that the perturbation factor f satisfies the linearized equation:

$$f_\tau + \mu f_{\xi\xi\xi} + \tfrac{3}{2}\mu(2v_0 v_{0\xi} f + v_0^2 f_\xi) = \rho k^2 \int_{-\infty}^{\xi} f. \tag{45}$$

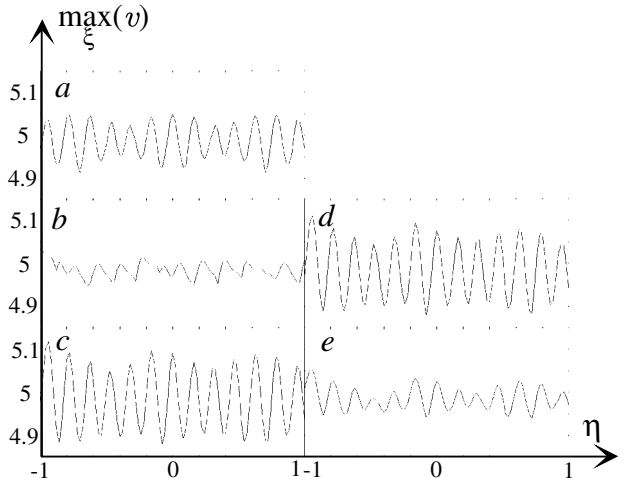

Figure 2. Plots of the maximal value of v against the transverse variable η. (*a*) Initial data, $v = 5\mathrm{sech}(2.5\xi + 1.25\eta - 1.25)(1 + 0.01\cos 40\eta)$. (*b*) After a time $\tau = 0.0025$ of evolution obeying equation (30), with $\rho = +1/4$. (*c*) After a time $\tau = 0.0025$ of evolution obeying equation (30), but $\rho = -1/4$. (*d*) After a time $\tau = 0.0025$ of evolution obeying the mKP equation (33) with $\rho = +1/4$. (*e*) After a time $\tau = 0.0025$ of evolution obeying equation (33), but $\rho = -1/4$. Other parameters: $\mu = 1$, $\nu = \mu/2$, $\gamma = 0$.

We assume that the oscillations are very fast, and thus k is very large. Then the ξ derivatives are negligible. Multiplying by $2f$, and then integrating with regard to ξ over $\mathbb{R}$, we obtain

$$\partial_\tau\left(\int_{-\infty}^{+\infty} f^2\,\mathrm{d}\xi\right) = \rho k^2\left(\int_{-\infty}^{+\infty} f\,\mathrm{d}\xi\right)^2. \tag{46}$$

Therefore the $\mathcal{L}^2$-norm of f is increasing with time if ρ is positive, decreasing when ρ is negative. This result has been checked numerically by solving equation (33) with the initial data (44), as shown in figures 2(*d*) and (*e*). It also appears to be valid for slower oscillations. The same result holds for the KP equation (32).

The stability depends thus on the sign of ρ in any case, but as for the kind of perturbation studied in the previous paragraph, the conclusions are inverse for equation (30) and for either the KP or the mKP equations. Taking into account the fact that ρ, and in practice also μ, are positive, we see that the complicated term involving the function Ψ, primitives, sine and cosine, destroys the stability of the line-soliton with regard to slow perturbations, while it ensures its stability with regard to fast oscillating perturbations in the physical situation considered.

4. Two-dimensional behaviour

4.1. Two line-solitons interacting

The line-soliton is, in some sense, a one-dimensional object. Properly multi-dimensional problems are, e.g., the existence of localized solutions, or the interaction of line-solitons. We consider first the latter question, using a numerical approach. The numerical resolution of equation (30) presents some difficulties that are detailed in appendix B, and that forced us to

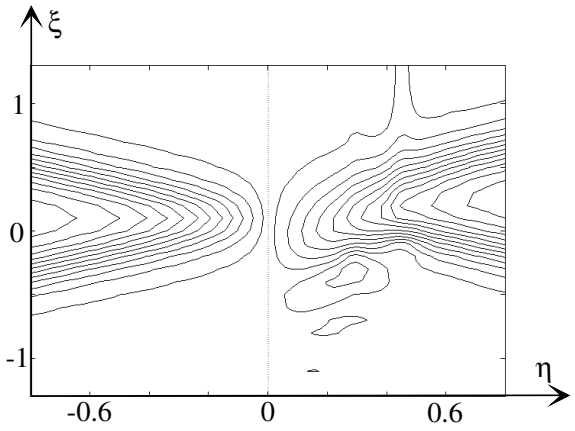

Figure 3. Contour plot of θ in the $\xi\eta$ plane. Left-hand side of the plot: initial data $v = 16(\mathrm{sech}(8\xi+4\eta-0.8)-\mathrm{sech}(8\xi-4\eta-0.8))$, right-hand side: after a propagation time $\tau = 0.0024$. Parameters: $\mu = 1$, $\rho = 1/4$, $\gamma = 0$.

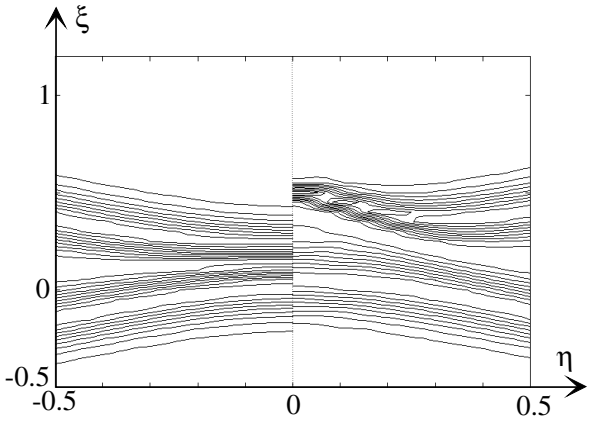

Figure 4. Contour plot of $\cos\theta$ in the $\xi\eta$ plane. Left-hand side of the plot: initial data $v = 16(\mathrm{sech}(8\xi + 4\eta - 0.8) + \mathrm{sech}(8\xi - 4\eta - 0.8))$, right-hand side: after a propagation time $\tau = 6.125 \times 10^{-4}$. Parameters: $\mu = 1$, $\rho = 1/4$, $\gamma = 0$.

restrict the study to two dimensions. The superposition of two line-solitons is given as initial data:

$$v_0 = \frac{2b}{\cosh(b(\xi - \xi_0) + c\eta)} \pm \frac{2b}{\cosh(b(\xi - \xi_0) + c\eta)}. \tag{47}$$

Notice that this choice satisfies $\lim_{\xi \longrightarrow +\infty} \theta \equiv 4\pi$, or 0, depending on the sign, justifying the use of a sum. Two sign cases are to be considered. The line-soliton solution describes a rotation of the magnetization density vector of a turn around the propagation direction. If the sign is +, the two solitons describe rotations in the same way. If the sign is −, the magnetization vector winds up in the first soliton, and unwinds in the second one. Both cases have been considered, yielding, after some propagation time, figures 3 and 4. The behaviour shows some common points in both situations. First, the two lines tend to separate from each other. The direction of the separation line changes: it is the η-axis in the winding up–unwinding case, and the ξ-axis

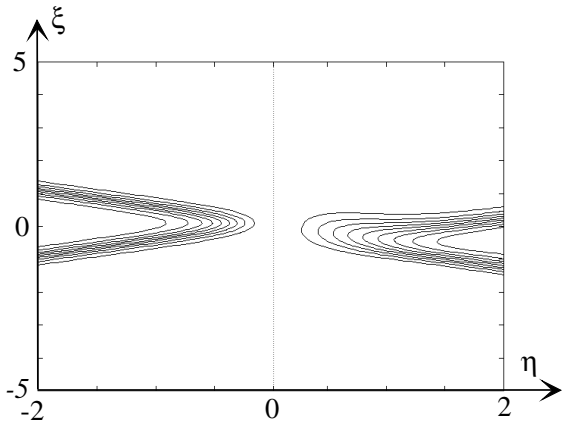

Figure 5. Contour plot of $\cos\theta$ in the $\xi\eta$ plane. Left-hand side of the plot: initial data $v = 4\mathrm{sech}(4(\xi - 0.1) + 2\eta) - 4\mathrm{sech}(4(\xi - 0.1) - 2\eta)$, right-hand side: after a propagation time $\tau = 0.032$. Parameters: $\mu = 1$, $\rho = 1/4$, $\gamma = -5$.

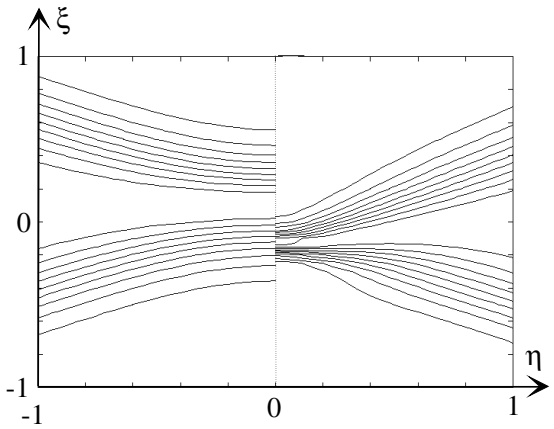

Figure 6. Contour plot of $\cos\theta$ in the $\xi\eta$ plane. Left-hand side of the plot: initial data $v = 4\mathrm{sech}(4(\xi - 0.1) + 2\eta) + 4\mathrm{sech}(4(\xi - 0.1) - 2\eta)$, right-hand side: after a propagation time $\tau = 0.0275$. Parameters: $\mu = 1$, $\rho = 1/4$, $\gamma = -5$.

otherwise. Second, instability appears, and $v = \theta_\xi$ blows up at some particular points. These points are always located on the back of the pulse and correspond to small concave parts of a globally convex line. There the variation of θ becomes very fast. The wave breaks due to the nonlinear velocity dispersion. We conclude that the initial data v_0 of equation (47) is unstable. It is not likely that the initial states used in figures 3 and 4 can be realized experimentally. Indeed, it would be produced *a priori* by two line-solitons that would have already propagated together during a long time. The simulation shows that the latter situation cannot occur.

4.2. Two interacting domain walls

The question considered here is the oblique interaction of two moving walls. Using the same numerical approach as above, we take as the initial data the linear superposition of two quasi-one-dimensional steady-state solutions, each being described by the roughly approximate

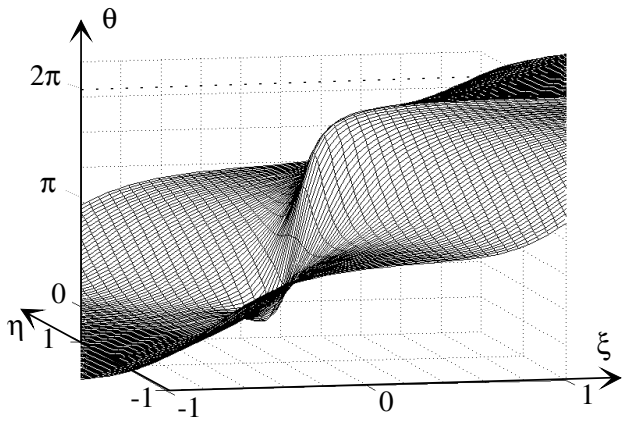

Figure 7. Mesh of θ versus ξ and η at $\tau = 0.0275$, for the same initial data and value of the parameters as in figure 6.

formula (34). The general expression of this initial data is thus the same as (47), but without the coefficient 2 on the numerators. Numerical resolution of equation (30) yields the results presented in figures 5 and 6. The conclusion is the same as in the case of line-solitons: interaction leads to breaking at the crossing. Thus two walls crossing each other cannot yield a self-similar, or weakly evolving, solution. The value of the magnetization precession angle θ in the moving wall, corresponding to figure 6, is shown in figure 7. The point where the wave breaks appears clearly. Other computations show that, in the case of two walls both rotating in the same direction, which is the case considered in figures 6 and 7, when damping is small enough, the region close to the crossing evolves to a line-soliton. The latter is unstable due to damping, and the same kind of breaking as shown in figure 6 finally occurs.

These features can be interpreted as follows: the domain wall thickness, either due to damping or to nonlinear instability, evolves toward its static equilibrium value, which is determined by the inhomogeneous exchange. But this value is rather small, while long waves are considered: it tends to zero in the long-wave approximation. This known equilibrium state is not smooth in the considered approximation, and the evolution toward it appears as a wave breaking.

4.3. Localized solution

A second truly multidimensional problem is that of the existence of stable localized solutions. Care must be taken in their definition: indeed, the magnetization density must be parallel to the external field out of the area occupied by the wave. Therefore, θ tends to zero at infinity in all directions, apart from an integer number of 2π. Not every function $v = \theta_\xi$ ensures this boundary condition. The energy of the pulse is roughly measured by its size, and the wave amplitude cannot vary: its value must be 2π, because the magnetization makes a complete turn (or π for a half turn in the case of a moving wall). Thus the pulse size must decrease during propagation, if damping is not negligible. The assumption that $\tilde{\sigma} = 0$ is thus a necessary condition for the existence of stable localized solutions. We make this assumption in the present section. Our approach is the following: we take some arbitrary initial data, but satisfying the correct boundary conditions at infinity, and examine whether it evolves to some stable state, or breaks up.

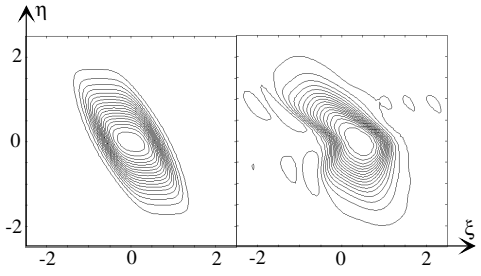

Figure 8. Contour plot of θ in the $\xi\eta$ plane. Left-hand side of the plot: initial data $v = 16e^{-\eta^2}(\mathrm{sech}(8\xi + 4\eta - 4.8) - \mathrm{sech}(8\xi + 4\eta + 4.8))$, right-hand side: after a propagation time $\tau = 0.0064$. Parameters: $\mu = 1$, $\rho = 1/4$, $\gamma = 0$.

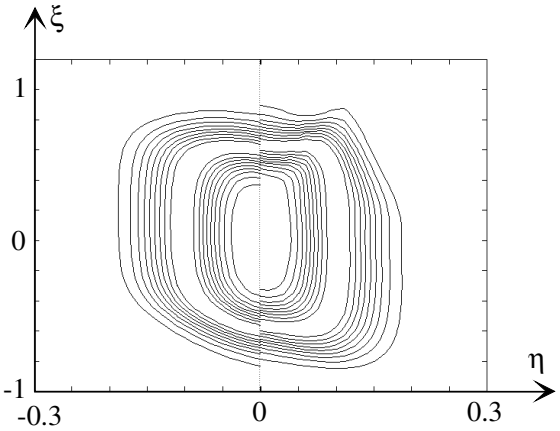

Figure 9. Contour plot of $\cos\theta$ in the $\xi\eta$ plane. Left-hand side of the plot: initial data $v = 16e^{-64\eta^2}(\mathrm{sech}8(\xi + \eta - 0.6) - \mathrm{sech}8(\xi + \eta + 0.6))$, right-hand side: after a propagation time $\tau = 6.5 \times 10^{-4}$. Parameters: $\mu = 1$, $\rho = 1/4$, $\gamma = 0$.

The following initial data v_0 has been considered:

$$v_0 = \left(\frac{2b}{\cosh(b(\xi - \xi_0) + c\eta)} - \frac{2b}{\cosh(b(\xi + \xi_0) + c\eta)}\right) e^{-\frac{\eta^2}{d^2}} \tag{48}$$

for various values of the constants, especially of d, that measures the size of the pulse in the η direction. For wide pulses, the behaviour is that shown in figure 8. It is seen that the centre of the wave travels faster than the sides, and the initially symmetrical plot takes an angular shape. Thus the pulse is not stable. This breaking is purely due to the nonlinear velocity dispersion; we have indeed checked that the same behaviour occurs when solving equation (30) with no transverse term ($\rho = 0$).

For a narrow pulse (d small), the effects of the transverse modulation term modifies strongly that of dispersion, and the above type breaking no longer arises, but another kind of instability occurs, as shown in figure 9. 'Horns' appear at the front of the pulse, while the rear becomes flat. Breaking will occur through the blow-up of the derivative v at the front of the pulse that will soon give rise to wave breaking.

No stable solution has appeared between these two extreme situations. Other computations have been done using other initial data, e.g. a Gaussian shape, or the KP I lump shape [10, p 209]. The same kind of wave breaking has occurred in any case, and we can conclude that the existence of stable localized solutions of equation (30) is unlikely.

4.4. About transverse collapse

Transverse collapse of a localized solution of the (3 + 1)-dimensional mKP equation (33) occurs under certain conditions, as shown in [14]. The question asks, whether the same behaviour arises with the model (30) studied in this paper. Because the proof in [14] rests on the Hamiltonian properties of equation (33), and system (30) is integro-differential, the analytical approach can hardly be generalized, and a numerical approach is required.

Let us first make precise the result of [14] about equation (33), adapted to the present notation and normalization. The discussion considers the parameters 'b' and 'D' that here are $-\mathrm{sgn}\rho$ and $+1$, respectively (μ being positive). The system possesses a conserved Hamiltonian, which is

$$\mathcal{H} = \frac{3}{16\mu^{1/3}} \int_{\mathbb{R}^3} \left(\mu v_\xi^2 - \rho(\theta_\eta^2 + \theta_\zeta^2) - \frac{\mu v^4}{4} \right) \mathrm{d}\xi \, \mathrm{d}\eta \, \mathrm{d}\zeta. \tag{49}$$

If both ρ and $\mathcal{H}$ are negative, the transverse momentum:

$$I = \int_{\mathbb{R}^3} (\eta^2 + \zeta^2) v^2 \, \mathrm{d}\xi \, \mathrm{d}\eta \, \mathrm{d}\zeta \tag{50}$$

becomes zero in a finite time, at most equal to

$$\tau_b = \frac{1}{\rho \mathcal{H}} \left(R_1 - \sqrt{R_2 - 16\rho R_2 \mathcal{H}} \right) \tag{51}$$

where $R_1 = \frac{\mathrm{d}}{\mathrm{d}\tau} I|_{\tau=0} = -2\rho \int_{\mathbb{R}^3} (\eta^2 + \zeta^2) v (\partial_\eta^2 + \partial_\zeta^2) \theta^2 \, \mathrm{d}\xi \, \mathrm{d}\eta \, \mathrm{d}\zeta|_{\tau=0}$ and $R_2 = I|_{\tau=0}$. The above integrals are computed easily for a Gaussian input $\theta = \theta_0 \exp -(\frac{\xi^2}{a^2} + \frac{\eta^2+\zeta^2}{b^2})$. It is found that

$$\tau_b = \sqrt{\frac{4\sqrt{2}}{3|\rho|\mu}} \frac{ab}{\sqrt{\theta_0^2 - \theta_{\mathrm{th}}^2}} \tag{52}$$

where

$$\theta_{\mathrm{th}} = \sqrt{32\sqrt{2} \left(1 + \frac{2}{3} \frac{a^4 |\rho|}{b^2 \mu} \right)} \tag{53}$$

is the amplitude threshold for the collapse. Let us give a numerical example: $\mu = 1$, $\rho = -1/4$, $\theta_0 = 12$, $a = 0.3$, $b = 0.035$. The chosen value of b minimizes τ_b, the other parameters keeping their values. Then $\tau_b = 0.0041$ is an upper bound of the blow-up time.

This instability is related to that of the line-solitons that also occurs for $\rho < 0$ in the case of the mKP equation (33). It has been shown in section 3 that, when the wave evolution is described by system (30), the line-solitons are unstable when $\rho > 0$ (the discussion and proof are given in 2 + 1 dimensions, but generalize easily to 3 + 1 dimensions). Therefore, blow-up is expected to arise for the same set of input data as above, but with $\rho = 1/4$ in equation (30). The pulse evolution is shown in figure 10(c). The input pulse is given in figure 10(a) and the evolution of the same pulse according to equation (33) in figure 10(b), for comparison. The self-focusing is the same, but another phenomenon appears, about $r = 0.02$ on the negative part of v. This corresponds to a wave emission toward the front (positive values of ξ), as discussed in the following section. This appears on the plot of θ (figure 10(d)) corresponding to the v of figure 10(c). It is comparable to the pulse of figure 9, discussed above.

This phenomenon leads quickly to numerical instability. Therefore the eventual continuation of self-focusing and collapse cannot be observed. We have not got numerical evidence for the collapse, because another kind of instability destroys the pulse, much more quickly than the collapse occurs in the three-dimensional mKP model (33).

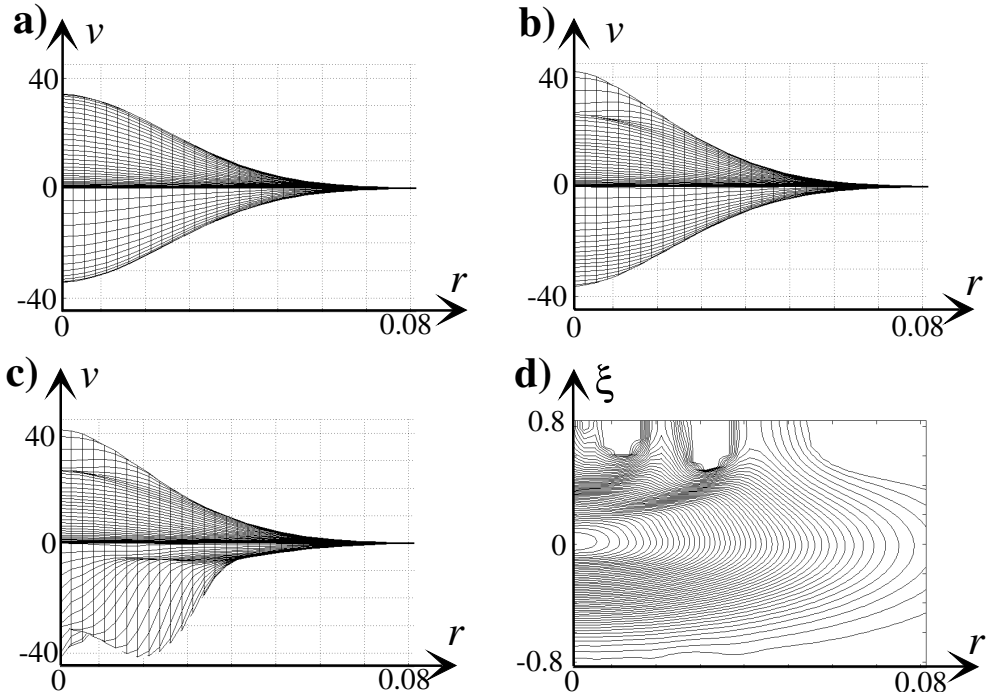

Figure 10. Three-dimensional evolution of a localized input: (*a*), (*b*), (*c*) mesh of v, seen from the rear ($\xi < 0$), (*a*) initial data, $v = \frac{-2\theta_0 x}{a^2} \mathrm{e}^{-\frac{x^2}{a^2} - \frac{r^2}{b^2}}$, $\theta_0 = 12$, $a = 0.3$, $b = 0.035$. (*b*) After a time $\tau = 0.72 \times 10^{-4}$ of evolution obeying the (3+1)-dimensional mKP equation (33) with $\rho = -1/4$. (*c*) After the same time of propagation as (*b*), but the wave evolution obeys equation (30) with $\rho = +1/4$. (*d*) Contour plot of θ under the same conditions as (*c*). Other parameters: $\mu = 1$, $\nu = \mu/2$. Damping is neglected.

5. Emission of a second wave

5.1. Observations on the simulations

If the two interacting line-solitons of figure 4 propagate further, a new wave is emitted toward the front, as shown in figure 11. This wave appears to propagate with an infinite velocity in the considered frame. This means that, in the frame moving at speed V, its propagation velocity V' is too fast to be described by the slow variables $\xi = \varepsilon(x - Vt)$ and $\tau = \varepsilon^3 t$. In other words, V' differs from V for more than a correction of the order of ε^2. The wave propagation mode to which the emitted wave belongs cannot be other than the other type of solitary wave that can exist in the medium, which we call the KdV mode. The latter propagates at a speed

$$V' = \sqrt{\frac{\alpha + \sin^2 \varphi}{1 + \alpha}}. \tag{54}$$

$V' > V$, thus such a wave is emitted toward the front. The difference $V' - V$ is finite when $\varepsilon \longrightarrow 0$, and therefore it appears to be infinite in the frame of the slow variables. From the technical point of view, it must be noticed that the boundary condition, that $\lim_{\xi \longrightarrow -\infty} \Psi = 0$, and so on, and the corresponding choice of primitives, renders impossible the emission of a wave towards the rear. It would have produced emission toward the front in the numerical

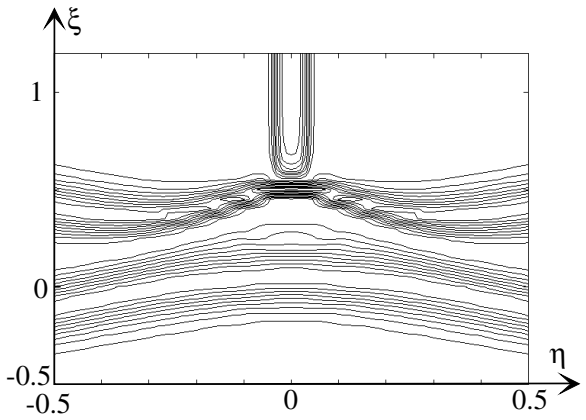

Figure 11. Contour plot of $\cos\theta$ in the $\xi\eta$ plane. Left-hand side of the plot: initial data $v = 16(\mathrm{sech}(8\xi + 4\eta - 0.8) + \mathrm{sech}(8\xi - 4\eta - 0.8))$, right-hand side: after a propagation time $\tau = 6.3125$. Note the emission of a wave toward the front.

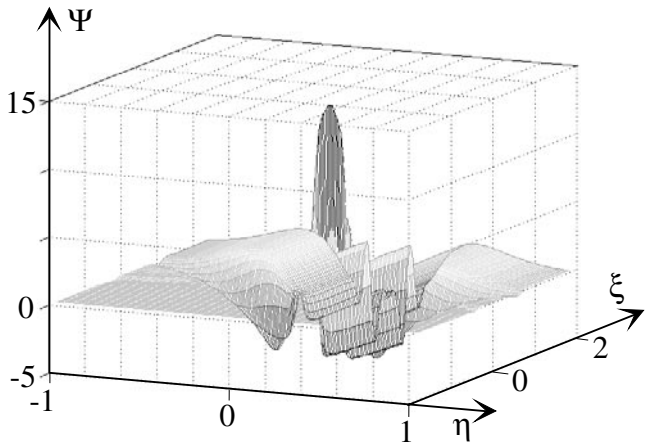

Figure 12. Mesh of Ψ corresponding to the θ plotted in figure 11 at the intermediary time $\tau = 5 \times 10^{-4}$. The initial data and the parameters are the same as in figure 11.

solution even if the physical situation were different. Thus the emission direction is determined by the fact that $V' > V$, and not really by the computation.

The emission originates in the transverse modulation term in the particular form it has here. Figure 12 shows a mesh of the function Ψ for the same parameters and initial data as in figure 4, but at a propagation time long before the breaking. A nonzero part of Ψ appears in front of the pulse. It is clearly due to the presence of an integration with regard to ξ in the expression of Ψ. It coincides with the location of the later forward emission. Thus the latter appears to be a consequence of the former.

5.2. A non-conservation law

The first conservation law of the mKdV equation (31) is that of the so-called pulse mass:

$$I = \int_{-\infty}^{+\infty} v \, \mathrm{d}\xi. \tag{55}$$

In the case of Nakata's soliton, the signification of this conservation law, $\partial_\tau I = 0$, differs from the usual interpretation of an abstract mKdV equation. Indeed, because $v = \theta_\xi$, and assuming that θ is zero as $\xi \longrightarrow -\infty$, we have $I = \lim_{\xi \longrightarrow +\infty} \theta$. Thus the condition, that θ is 2π as $\xi \longrightarrow +\infty$ which must be satisfied in a saturated medium, can be realized only if I is conserved.

Let us examine what happens to this conservation law when the transverse modulation is taken into account. We neglect damping, i.e. we consider equation (30) with $\gamma = 0$. Obviously, $\partial_\tau I = \int_{-\infty}^{+\infty} v_\tau \, \mathrm{d}\xi$. The derivative v_τ is computed from equation (30) and integrated. We assume that all longitudinal derivatives of θ vanish at infinity (that is, $\partial_\xi^k v \longrightarrow 0$ as $\xi \longrightarrow +\infty$ for all $k \geqslant 0$). Then the integrals of the dispersion and nonlinear terms vanish, and $\partial_\tau I$ reduces to

$$\partial_\tau I = \rho \int_{-\infty}^{+\infty} \left(v_\xi \int_{-\infty}^{\xi} \Psi \, \mathrm{d}\xi' + 2v\Psi - \int_{-\infty}^{\xi} \Delta v \, \mathrm{d}\xi' \right) \mathrm{d}\xi. \tag{56}$$

An integration by parts shows that

$$\int_{-\infty}^{+\infty} \left(v_\xi \int_{-\infty}^{\xi} \Psi \, \mathrm{d}\xi' + v\Psi \right) \mathrm{d}\xi = \lim_{\xi \longrightarrow +\infty} v \int_{-\infty}^{\xi} \Psi \, \mathrm{d}\xi' \tag{57}$$

where Ψ involves primitives of transverse derivatives of bounded functions. Although it is not a necessary mathematical condition, it is reasonable to assume that these transverse derivatives are also bounded with regard to ξ. Thus Ψ is at most linear with regard to the same variable, and $\int_{-\infty}^{\xi} \Psi \, \mathrm{d}\xi'$ grows at least as fast as ξ^2. On the other hand, v decreases exponentially in the case of the soliton. Thus it can be reasonably assumed that $\int_{-\infty}^{\xi} \Psi \, \mathrm{d}\xi'$ grows slower than $1/v$ as $\xi \longrightarrow +\infty$, and the value of expression (57) is zero.

The terms remaining in equation (56) are evaluated using equation (29), keeping in mind that $\theta_\xi = v$, to yield

$$\partial_\tau I = -\rho \lim_{\xi \longrightarrow +\infty} \Phi. \tag{58}$$

We have made use of the fact that $\lim_{\xi \longrightarrow -\infty} \Phi = 0$. If we assume further that $\lim_{\xi \longrightarrow +\infty} \theta$ is a integer multiple of 2π, we can make expression (58) a little more explicit:

$$\partial_\tau I = -\rho \int_{-\infty}^{+\infty} \Delta \sin\theta \, \mathrm{d}\xi. \tag{59}$$

Thus the quantity I is no longer conserved when $\Delta \sin\theta$ is not zero on average. The energy loss of the pulse, related to the emission of another wave, originates in this non-conservation law.

6. Conclusion

Our initial purpose was to complete the theory of [3] and [4] by studying the effect of transverse perturbations on it. Let us first look at results obtained in this paper from this mainly mathematical point of view. First, the three-dimensional generalization of the mKdV equation obtained by Nakata is not, as could be naively expected, the mKP equation (33), but some complicated integro-differential equation, equation (30). Second, this equation admits line-soliton solutions, whose stability properties have been determined. The dependency of this stability with regard to the coefficients of equation (30), mainly the product $\mu\rho$, is in contrast to what happens for the KP and mKP equations, which was already well established. Third, numerical simulations have shown that wave breaking occurs when the transverse variations are important: oblique interaction of line-solitons and eventual localized solutions. Fourth,

even the first conservation law of the mKdV equation is not satisfied in more than (1 + 1) dimensions.

Physical consequences can be drawn from these mathematical results. The domain walls and Nakata's solitons are very unstable with regard to transverse perturbations, except for very fast transverse oscillations. This instability is able to yield the emission of a new wave, which appears to belong to the other solitary wave mode supported by the medium, that was called the KdV mode in [5]. In a way comparable to the emission of a high-frequency wave by an oscillating domain wall [2], a solitary wave can arise from the slow transverse modulations of such a wall. Thus this theoretical study gives a way to produce experimentally waves of the KdV mode that have been theoretically predicted but never observed, to my knowledge.

Appendix A. Line-soliton stability

We give here the detail of the proof of the stability conditions mentioned in section 3.2.2. We consider the multiscale expansion defined by equations (40)–(42). At order δ^0 the equation obtained states that $v^{(0)}$ satisfies the mKdV equation (31). At order δ^n it is

$$\mathcal{L}v^{(n)} = \mathcal{F}^{(n)} \tag{60}$$

with

$$\mathcal{L}v^{(n)} = -\mu\lambda^2 v_X^{(n)} + \frac{3\mu}{2}(v^{(0)2}v^{(n)})_X + \mu v_{XXX}^{(n)}. \tag{61}$$

For $n = 1$, the right-hand side is $\mathcal{F}^{(1)} = -\partial_T v^{(0)} = v_X^{(0)}\xi_T^{(0)}$, and a solution of equation (60) is found explicitly:

$$v^{(1)} = \frac{\xi_T^{(0)}}{2\mu\lambda^2}(v^{(0)} + Xv_X^{(0)}). \tag{62}$$

For $n = 2$, we have

$$\mathcal{F}^{(2)} = -\partial_T v^{(1)} - \frac{3\mu}{2}(v^{(1)2}v^{(0)})_X + \rho\left(v_X^{(0)}\int_{-\infty}^{X}\Psi^{(2)}\,\mathrm{d}X' + 2v^{(0)}\Psi^{(2)} - \int_{-\infty}^{X} v_{YY}^{(0)}\,\mathrm{d}X'\right) \tag{63}$$

where $\Psi^{(2)}$ is the coefficient of δ^2 in the expansion of Ψ in powers of δ.

The adjoint operator of $\mathcal{L}$ is $\mathcal{L}^*$, defined by

$$\mathcal{L}^*u = \mu\lambda^2 u_X - \frac{3\mu}{2}v^{(0)2}u_X - \mu u_{XXX}. \tag{64}$$

It is noticed that $\mathcal{L}^*v^{(0)} = 0$, and thus $v^{(0)}\mathcal{L}v^{(2)} - v^{(2)}\mathcal{L}^*v^{(0)} = v^{(0)}\mathcal{F}^{(2)}$, and the condition under which $v^{(0)}$ remains bounded is

$$\int_{-\infty}^{+\infty} v^{(0)}\mathcal{F}^{(2)}\,\mathrm{d}X' = 0. \tag{65}$$

All works as in [13], except the contribution of Ψ, which is specific to equation (30). Obviously, $\Psi^{(2)}$ has the same expression as (35) for Ψ, but keeping only the leading order $\theta^{(0)} = \int_{-\infty}^{X} v^{(0)}\,\mathrm{d}X'$ of θ, and using Y derivatives instead of η derivatives. They give

$$w_{YY} = w_{XX}\,\xi_Y^{(0)2} - w_X\,\xi_{YY}^{(0)} \tag{66}$$

as well for $w = \sin\theta^{(0)}$ as for $w = \cos\theta^{(0)}$. Taking care of the limit when $X \longrightarrow -\infty$, we obtain

$$\Psi^{(2)} = (\cos\theta^{(0)} - 1)\xi_{YY}^{(0)}. \tag{67}$$

The integral in (65) is then computed, noticing that the odd functions have a zero contribution. The term involving a primitive of $\Psi^{(2)}$ is incorporated into the neighbour using integration by parts. This gives

$$\int_{-\infty}^{+\infty} v^{(0)}\mathcal{F}^{(2)}\,\mathrm{d}X' = \frac{-\xi_{TT}^{(0)}}{4\mu\lambda^2}\int_{-\infty}^{+\infty} {v^{(0)}}^2\,\mathrm{d}X' + J\rho\xi_{YY}^{(0)} \tag{68}$$

with

$$J = \left(\tfrac{3}{2}\int_{-\infty}^{+\infty} {v^{(0)}}^2(\cos\theta^{(0)} - 1)\,\mathrm{d}X' + \int_{-\infty}^{+\infty} {v^{(0)}}^2\,\mathrm{d}X'\right). \tag{69}$$

The condition $\int_{-\infty}^{+\infty} v^{(0)}\mathcal{F}^{(2)}\,\mathrm{d}X' = 0$ yields the evolution equation (43) for $\xi^{(0)}$.

The crucial point is the sign of J. Using the following explicit expression of $\cos\theta^{(0)}$, equivalent to (39) and given in [3]:

$$\cos\theta^{(0)} = 1 - 2\mathrm{sech}^2\lambda X \tag{70}$$

and the explicit expression (38) of $v^{(0)}$, we get $J = 4\lambda(\int_{-\infty}^{+\infty}\mathrm{sech}^2 r\,\mathrm{d}r - 3\int_{-\infty}^{+\infty}\mathrm{sech}^4 r\,\mathrm{d}r)$. The value of the two latter integrals are, respectively, 2 and $4/3$, and thus $J = -8\lambda$.

Thus the soliton is stable when $\mu\rho$ is negative and unstable when $\mu\rho$ is positive. The proof coincides with that of [13] for KP, except for the terms involving Ψ. Regarding the mKP equation (33), all is the same, except that Ψ must be replaced by 0, and thus J by $J_0 = \int_{-\infty}^{+\infty} {v^{(0)}}^2\,\mathrm{d}X' = +8\lambda$. Thus the sign in (43) is changed, and the conclusions are inverted. The latter then coincide exactly with those given by [13] for the KP equation (32).

Appendix B. Numerical computations

We give here an account of the numerical techniques used to solve the asymptotic equation derived in section 2 of this paper. Due to several difficulties, we restrict to $(2+1)$ dimensions, and will neglect the damping ($\gamma = 0$) in a first stage. Despite that a finite difference scheme for the purely differential system (27)–(29) for the three unknown functions F, Φ and θ can be written, it fails to converge, at least for the accessible computation time and memory size. A fixed point algorithm using Fourier transforms can be considered.

But θ does not vanish at infinity with regard to the transverse variable η, and neither does v. Thus only a Fourier transform with regard to ξ can be used. Further, the θ function does not vanish either as ξ tends to $+\infty$, at least for the one-line-soliton solution. Thus the Fourier transform cannot be used for the integrations with regard to ξ. This makes the algorithm rather complex and very lengthy, but it allows us to obtain some results.

The algorithm used is as follows: we want to solve the system (30)–(35) with the initial data

$$v(\xi, \eta, \tau = 0) = v_0(\xi, \eta). \tag{71}$$

Notice that equation (35) is an explicit expression for Ψ, and therefore does not involve initial Cauchy data for this function. We build some recurrent sequence of functions v_n, Ψ_n, θ_n, solving for each n the following Cauchy problem:

$$\partial_\tau v_{n+1} + \mu\partial_\xi^3 v_{n+1} + \tfrac{3}{2}\mu v_n^2\partial_\xi v_n - \rho\left(\partial_\xi v_n\int_{-\infty}^{\xi}\Psi_n\,\mathrm{d}\xi' + 2v_n\Psi_n\right) = \rho\int_{-\infty}^{\xi}\partial_\eta^2 v_n\,\mathrm{d}\xi' \tag{72}$$

together with the initial data (71), and the definition (35) of Ψ, θ being defined by $\theta = \int_{-\infty}^{\xi} v\,\mathrm{d}\xi'$. Equation (72) is linear and can be solved by Fourier analysis. We define the Fourier transform $\mathcal{F}(F) = \hat{F}$ of any function F by

$$F(\xi, \eta, \tau) = \int_{\mathbb{R}} \hat{F}(k, \eta, \tau)\mathrm{e}^{2\mathrm{i}\pi k\xi}\,\mathrm{d}\xi. \tag{73}$$

Then the evolution equation of the system (72) is solved as

$$\hat{v}_{n+1} = \left[\hat{v_0} + \int_0^t \mathcal{F}(\mathcal{U})\mathrm{e}^{-8\mathrm{i}\pi^3\mu k^3\tau'}\,\mathrm{d}\tau'\right]\mathrm{e}^{8\mathrm{i}\pi^3\mu k^3\tau} \tag{74}$$

with

$$\mathcal{U} = -3\nu v_n^2\partial_\xi v_n + \rho\left(\partial_\xi v_n \int_{-\infty}^{\xi} \Psi_n\,\mathrm{d}\xi' + 2v_n\Psi_n - \int_{-\infty}^{\xi} \partial_\eta^2 v_n\,\mathrm{d}\xi'\right). \tag{75}$$

The ξ primitives are simply computed through an approximation of the area trapezoids, and the η derivatives through a three-point finite-difference algorithm. The problems on the η boundary are avoided by the use of the four-point algorithm

$$\partial_\eta^2\theta_1 = [2\theta_1 - 5\theta_2 + 4\theta_3 - \theta_4]/\delta\eta^2 + \mathrm{O}(\delta\eta^4) \tag{76}$$

where $\theta_j = \theta(\eta_0 + (j-1)\delta\eta)$, at one end, and the analogous term at the other.

The fixed point of the sequence $(v_n)_n$ is the solution of the Cauchy problem. The numerical scheme converges only for a value of τ less than some bound. When this maximum is less than the desired propagation distance, the same scheme is repeated several times along the propagation.

When damping is taken into account, equations (74) and (75) are modified in three ways:

- The phase factor $8\mathrm{i}\pi^3\mu k^3$ is replaced by $8\mathrm{i}\pi^3\mu k^3 + 4\pi^2\gamma k^2$.
- The integral $\int_{-\infty}^{\xi} \Psi_n\,\mathrm{d}\xi'$ is replaced by $\int_{-\infty}^{\xi}(\Psi_n\,\mathrm{d}\xi' - \frac{\gamma}{\rho}v_n^2)$.
- A supplementary nonlinear term $-\gamma v_n^3$ is added to the expression (75) of $\mathcal{U}$.

In contrast to the line-solitons, localized solutions vanish as $\eta \longrightarrow \pm\infty$. This allows the use of a Fourier transform with regard to η for the computation of the derivatives $\partial_\eta^2\theta$, $\partial_\eta^2 \sin\theta$ and $\partial_\eta^2 \cos\theta$. This gives an algorithm which is a little faster and is used in the computations of sections 3 and 4.

References

[1] Bass F G and Nasonov N N 1990 Nonlinear electromagnetic-spin waves *Phys. Rep.* **189** 165

[2] Bass F G, Nasonov N N and Naumenko O V 1988 Dynamics of a Bloch wall in a magnetic field *Sov. Phys.–Tech. Phys.* **33** 742–8

[3] Nakata I 1991 Nonlinear electromagnetic waves in a ferromagnet *J. Phys. Soc. Japan* **60** 77

[4] Nakata I 1991 Shock waves in a ferromagnet *J. Phys. Soc. Japan* **60** 2179

[5] Leblond H 1995 Interaction of two solitary waves in a ferromagnet *J. Phys. A: Math. Gen.* **28** 3763–84

[6] Leblond H 1996 Electromagnetic waves in ferrites: from linear absorption to the nonlinear Schrödinger equation *J. Phys. A: Math. Gen.* **29** 4623–39

[7] Bozorth R M 1951 *Ferromagnetism* (Princeton, NJ: Princeton University Press)

[8] De Gasperis P, Marcelli R and Miccoli G 1987 Magnetostatic soliton propagation at microwave frequency in magnetic garnet films *Phys. Rev. Lett.* **59** 481

[9] Cottam M G (ed) 1994 *Linear and Nonlinear Spin Waves in Magnetic Films and Superlattices* (Singapore: World Scientific)

[10] Ablowitz M J and Clarkson P A 1991 *Solitons, Nonlinear Evolution Equations and Inverse Scattering* (Cambridge: Cambridge University Press)

[11] Whitham V 1974 *Linear and Nonlinear Waves* (New York: Wiley)

[12] Landau L and Lifchitz E 1935 On the theory of dispersion of magnetic permeability in ferromagnetic bodies *Phys. Z. Sowj.* **8** 153

[13] Ablowitz M J and Segur H 1981 *Solitons and the Inverse Scattering Transform* (Philadelphia: SIAM)

[14] Turitsyn S K and Fal'kovitch G E 1985 Stability of magnetoelastic solitons and self-focusing of sound in antiferromagnets *Sov. Phys.–JETP* **62** 146–52